Enzymatically-Active Nanoparticles to Direct the Self-Assembly of Peptides in Hydrogel With a 3D Spatial Control

Miryam Criado-Gonzalez, Jean-Yves Runser, Alain Carvalho, Fouzia Boulmedais, Pierre Weiss, Pierre Schaaf, Loïc Jierry

Enzymatically-Active Nanoparticles to Direct the Self-Assembly of Peptides in Hydrogel With a 3D Spatial Control

Miryam Criado-Gonzalez,[a,b] Jean-Yves Runser,[a,b,c] Alain Carvalho,[a] Fouzia Boulmedais,[a] Pierre Weiss,[d] Pierre Schaaf,[a,b,c]* and Loïc Jierry,[a]**

a. Université de Strasbourg, CNRS, Institut Charles Sadron UPR 22, 67034 Strasbourg, France.

b. Institut National de la Santé et de la Recherche Médicale, UMR-S 1121, "Biomatériaux et Bioingénierie", 67087 Strasbourg, France.

c. Université de Strasbourg, Faculté de Chirurgie Dentaire, Fédération de Médecine Translationnelle de Strasbourg and Fédération des Matériaux et Nanoscience d'Alsace, 67000 Strasbourg, France.

d. Université de Nantes, ONIRIS, INSERM UMR 1229, 1 place Alexis Ricordeau, 44042 Nantes, France.

ABSTRACT

Hydroxypropylmethylcellulose grafted with silanol groups (Si-HPMC) hydrogels are employed as 3D scaffolds to encapsulate phosphatase-modified silica nanoparticles (AP@NPs). Such hybrid materials are catalytically active when enzyme susbtrates are diffusing through the material. Using the enzyme-assisted self-assembly concept, the tripeptide Fmoc-FFY is generated *in situ* in close vicinity of AP@NPs thanks to the phosphate hydrolysis of the diffusing precursor Fmoc-FF*p*Y. The self-assembly of Fmoc-FFY is spatially concomitant to the presence of AP@NPs. In the Si-HPMC host hydrogel, AP@NPs aggregate and thus limit their diffusion in the material. This feature is used to localize at the micrometer scale the self-assembly within the material: AP@NPs are injected in a defined 3D area within the Si-HPMC gel using an adapted microsyringe. The diffusion of precursor Fmoc-FF*p*Y toward this region leads to a Fmoc-FFY self-assembly exclusively there, an impossible strategy using free AP. Thus, this work allows to spatially control the enzyme-assisted self-assembly of peptides within host materials as an alternative approach for the design of hierarchically structured materials.

1. Introduction

Hydrogels, three-dimensional networks able to hold a large amount of water, receive great attention for several applications, *i.e.*, drug delivery, bio-immobilization, waste water treatment, or sustainable energy storage, among others [1-5]. In this regard, the design of hydrogels with controlled structures is a key role to modulate their final properties, which will in turn target their application. Polymers have been widely employed for the fabrication of 3D networks with different mesh size, swelling behavior, and mechanical properties. However, in some cases they are lack of biological functionality, which can be overcome by the design of hybrid hydrogels combining polymers and sequence-defined peptides [6-8].

Enzyme-assisted self-assembly (EASA) is an interesting approach for the transformation of low molecular weight precursors into hydrogelators, which then self-assemble leading to a supramolecular hydrogel [9-11]. Moreover, EASA allows the self-assembly localization where the enzyme is spatially located, through the covalent grafting of suitable enzymes on a glass substrate [12]. Thus, the self-assembly takes place in the spatial regions where both the precursors and the enzymes are present simultaneously [13]. We and others have developed localized EASA (or LEASA) on surfaces with various types of enzyme-triggered processes and on various kinds of substrates whatever their shape and their size (planar surfaces, nanoparticles or porous structures) [14-21]. Recently, it was reported that the self-assembly of precursors can be effective within a host material such as polymer hydrogels. This was highlighted by van Esch [22, 23] and Smith [24, 25] using protons as trigger of the precursor self-assembly within agarose or calcium alginate hydrogels. Indeed, the diffusion of precursor compounds at a specific area within a proton-loaded host gel directs the self-assembly process in the targeted area. Our group has shown that EASA can be an interesting tool to initiate molecular self-assembly within polymeric host hydrogels

containing an embedded enzyme as a trigger of peptides self-assembly [26], and modulate thus the cell adhesion properties of the so-designed substrate [27]. Very recently, the diffusion of precursor peptides within a host hydrogel has been shown to also induce the spontaneous micropatterning of self-assembled peptides zones, highlighting the potential of LEASA for autonomous 3D microstructuration of soft materials [28]. This is one aspect of particular relevance for the current development of biomaterials [29]. However, in spite of these promising developments of a new bottom-up approach to design structured functional materials, all works in this field suffers from the diffusion of the triggers, *i.e.*, enzymes or protons, in the material so that their localization in a restricted area within the material is impossible. Compared to protons, enzymes can be covalently immobilized within the host hydrogel through a covalent grafting along the constitutive polymer chains of the material. This is usually performed by diffusion of chemically-modified enzymes within a hydrophilic host gel. But this strategy is not without disadvantages [30-32]: First, polymer hydrogels are prepared from few %w/v of polymer chains resulting in a low density of grafted enzymes. Second, it is highly difficult to remove from the gel both the non-grafted enzymes and potential secondary compounds coming from the enzyme grafting reaction. Herein we present an alternative approach based on the use of encapsulated alkaline phosphatase-conjugated nanoparticles (NPs@AP) in a silanized hydroxypropylmethylcellulose (Si-HPMC) host hydrogel. We have studied the impact of the NPs@AP within the Si-HPMC gel and the resulting EASA of Fmoc-FFY from the phosphorylated precursors Fmoc-FF*p*Y diffusion through the host polymer material (Scheme 1). In addition, the 3D localization of peptides self-assembly in a defined spatial area of the Si-HPMC hydrogel (LEASA) is illustrated through the syringe injection of NPs@AP within the precursor peptide contained-host material using confocal laser scanning microscopy (CLSM) leading to complex microstructured patterns.

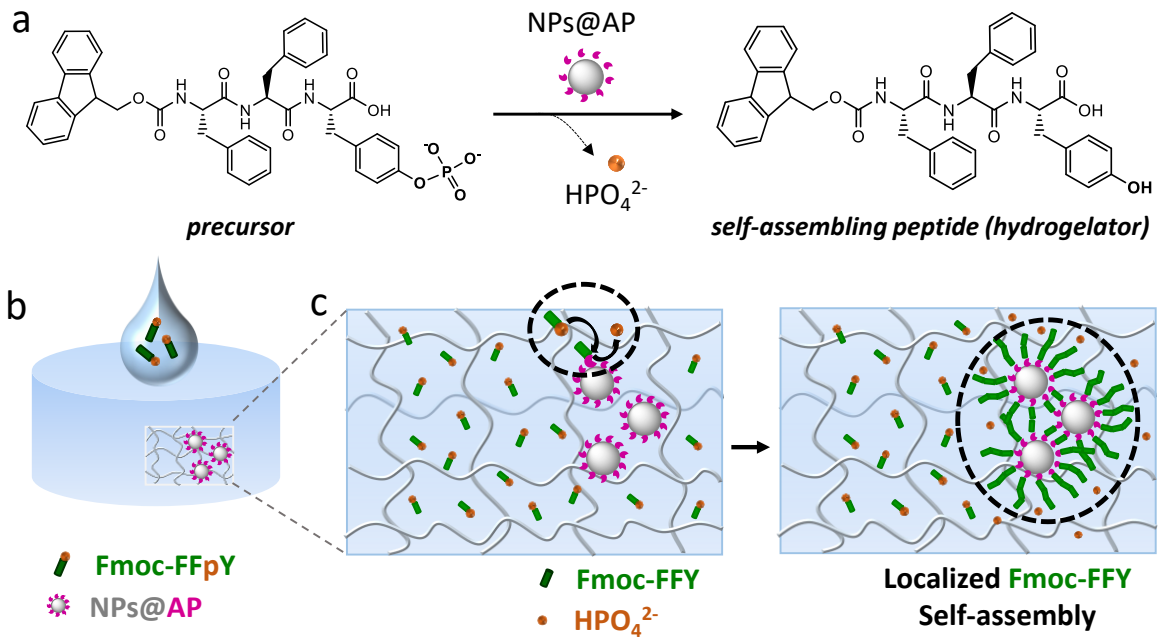

Scheme 1. (a) Phosphate group hydrolysis of the precursor Fmoc-FF*p*Y leading to the self-assembling tripeptide Fmoc-FFY catalysed by NPs@AP. (b) Precursor solution of Fmoc-FF*p*Y is brought in contact with the host hydrogel containing NPs@AP. (c) Fmoc-FF*p*Y diffuses inside the material and is enzymatically transformed in Fmoc-FFY leading to localized Fmoc-FFY self-assembly in close vicinity of NPs@AP.

2. Materials and Methods

2.1. Materials

Alkaline phosphatase from bovine intestinal mucosa (AP) (10 DEA units mg^{-1} protein), *para*-Nitrophenyl Phosphate Liquid Substrate System (PNP), tetraethyl orthosilicate (TEOS), (3-glycidyloxypropyl), and trimethoxysilane (GPMS) were purchased from Sigma Aldrich. Dry toluene and sodium tetraborate anhydrous (borax) were provided by Acros Organics, ammonium hydroxide by Carlo Erba, and ethanol by VWR. Fmoc-FF*p*Y (99% purity, natural chirality) was provided by PepMic and its characterization was identical to a previous reported work [19].

2.2. Synthesis of silica nanoparticles, NPs, NPs@AP, NPs@AP^{RHO}

Silica nanoparticles (NPs) and alkaline phosphatase immobilized nanoparticles (NPs@AP) were synthetized according to the procedure described previously [33]. The same procedure was employed for the covalent grafting of AP^{RHO} (AP was previously labelled with rhodamine B according to a reported procedure) [34] leading to NPs@AP^{RHO}. The average size of the nanoparticles was obtained by transmission electron microscopy (TEM), ~120 nm, and dynamic light scattering (DLS), ~135 nm.

2.3. Preparation of 1.5%w/v Si-HPMC hydrogels and Fmoc-FFpY diffusion in this host hydrogel

Triethoxypropyl-modified hydroxypropylmethylcellulose, called Si-HPMC, has been prepared according to the reported procedure [35]. Si-HPMC hydrogels were prepared by mixing 100 µL of Si-HPMC solution at 3%w/v in NaOH 0.1M and pH 12.9 with 100 µL of HEPES buffer at pH 3.6 in a vortex and let them gelate at room temperature. In the case of Si-HPMC with nanoparticles embedded, *i.e.,* Si-HPMC/NPs@AP, 20 µL of NPs or NPs@AP solutions were centrifuged at 13500 rpm for 10 min and redispersed in 100 µL of Si-HPMC solution at 3%w/v in NaOH 0.1M and pH 12.9 by mechanical stirring. Then, 100 µL of HEPES buffer at pH 3.6 was added, vortexed and let them gelate at room temperature. For the Fmoc-FF*p*Y diffusion tests, after 48 hours gelation, 100 µL of Fmoc-FF*p*Y solution (2.5 mg mL^{-1} in borax buffer) was added on top, and let in contact for 48 h at room temperature. For localized Fmoc-FFY self-assembly experiments, after 48h Si-HPMC gel formation, 1 µL of NPs or NPs@AP solutions (0.6 µg mL^{-1} in borax buffer 25 mM) was injected with a microsyringe through the lateral section of the Si-HPMC host hydrogel. After the introduction of the beveled needle within the Si-HPMC hydrogel, the syringe was gently retracted concomitantly of the application of a slight pressure on the plunger to release the NPs@AP in microcracks formed.

2.4. UV spectroscopy

The AP activity from NPs@AP embedded inside the Si-HPMC hydrogels was measured in an UV spectroscopy microplate reader (FLX-Xenius®, SAFAS, Monaco). Samples were incubated with 200 µL of *para*-nitrophenylphosphate (PNP) at 1 mM in borax buffer, which yields a yellow colour with absorbance at λ = 405 nm due to *para*-nitrophenol formation.

2.5. Infrared spectroscopy

Infrared spectra were recorded from 800 to 4000 cm^{-1} at 2 cm^{-1} resolution using a Vertex 70 spectrometer (Bruker, Germany), a DTGS detector, and the software Bruker OPUS/IR (version 7.5).

2.6. Fluorescence spectroscopy

Samples were prepared in a special 96 well plate and fluorescence spectra were recorded with a microreader fluorescence spectroscope (FLX-Xenius®, SAFAS, Monaco) using an excitation wavelength of 290 nm.

2.7. Rheology measurements

Hydrogels were prepared in Teflon molds of 10 mm diameter by mixing 100 µL of Si-HPMC solution at 3%w/v in NaOH 0.1M and pH 12.9 with 100 µL of HEPES buffer at pH 3.6 in a vortex and let them gelate at room temperature. In the case of Si-HPMC with nanoparticles embedded, 20 µL of NPs@AP solution were centrifuged at 13500 rpm for 10 min and redispersed in 100 µL of Si-HPMC solution at 3%w/v in NaOH 0.1M and pH 12.9 by mechanical stirring. Then, 100 µL of HEPES buffer at pH 3.6 was added, vortexed and let them gelate at room temperature. After different gelation times, dynamic oscillatory rheology was carried out in a Kinexus Malvern rheometer at 25°C. A stainless stell sandblasted plate geometry of 10 mm diameter was employed,

and a gap of 2 mm was fixed. Strain sweeps, from 0.01% to 100%, were performed at 1 Hz, and frequency sweeps, from 0.01 Hz to 10 Hz, were carried out at 0.1% strain.

2.8. Confocal laser scanning microscopy (CLSM)

50 µL of Si-HPMC solution at 3%w/v in NaOH 0.1M and pH 12.9 was mixed with 50 µL of HEPES buffer at pH 3.6 in a vortex and let them gelate at room temperature for 48 hours in Teflon molds of 10 mm diameter. In the case of Si-HPMC with nanoparticles embedded, 10 µL of NPs@AP with a 10 %v/v NPs@AP^{RHO} (AP^{RHO}, AP labelled with rhodamine B was prepared according to a reported procedure) [34] was centrifuged at 13500 rpm for 10 min and redispersed in 50 µL of Si-HPMC solution at 3%w/v in NaOH 0.1M and pH 12.9 by mechanical stirring. Then, 50 µL of HEPES buffer at pH 3.6 was added, vortexed and let them gelate at room temperature. After 48 h gel formation, 50 µL of Fmoc-FF*p*Y (2.5 mg mL^{-1}) containing Thioflavin T (0.45 mg mL^{-1}) was brought in contact with Si-HPMC hydrogels for 48 h at room temperature. Confocal laser scanning microscopy was performed with a Zeiss LSM 710 microscope using two objectives, an EC Plan-Neofluar 10x/0.3 and a Plan-Apochromat 20x/0.8 M27. The fluorescence emission of rhodamine between 566 and 703 nm was measured after excitation at 561 nm, whereas the peptide self-assembly using Thioflavine T (0.45 mg mL^{-1}) was visualized between 493 and 548 nm after excitation at 488 nm with an argon laser. The setup for samples preparation and measurement is shown in the Fig. S9.

2.9. Cryo-Scanning Electron Microscopy (Cryo-SEM)

A slight piece of Si-HPMC or Si-HPMC/NPs@AP gel was immersed in liquid ethane and fixed in a cryo-holder plunged into a nitrogen bath as described previously [36]. Then, the holder was placed into the cryo preparation chamber of the Quorum PT 3010 equipment under vacuum,

fractured with a razor blade, and transferred to the FEG-cryoSEM (Hitachi SU8010) to be observed at 1kV and -150°C.

3. Results and discussion

Si-HPMC hydrogel is an interesting biomaterial since it is fully biocompatible, and cells can live in a quiescent state during three weeks at least [35]. It is a chemical hydrogel based on siloxane bonds crosslinking between triethoxysilane-modified cellulose chains [37]. For our study, a 1.5%w/v Si-HPMC hydrogel was investigated. As model system of EASA, we have used the following couple composed of the precursor peptide Fmoc-FF*p*Y [14, 38] and NPs@AP prepared according to a reported procedure [33] (Scheme 1a). The NPs@AP have an average diameter of 120 nm and all traces of unbounded AP have been removed (Fig. S1 in supporting information). Recently, we have shown that NPs@AP can effectively trigger the Fmoc-FFY self-assembly in solution which exhibits antimicrobial properties [39]. The presence of 0.1% NPs@AP does not preclude the gelation of the Si-HPMC host hydrogel as shown by the inverted tube test picture given in Fig. 1a and Fig. S2. The hydrogel obtained is slightly light grey due to the presence of NPs@AP, compared to the translucent naked Si-HPMC gel, *i.e.*, without NPs@AP. The morphology of this hybrid hydrogel was analysed by cryo-SEM (Fig. 1b) observing the presence of clusters of micrometre-size nanoparticles within the fibrillar network of the Si-HPMC gel network.

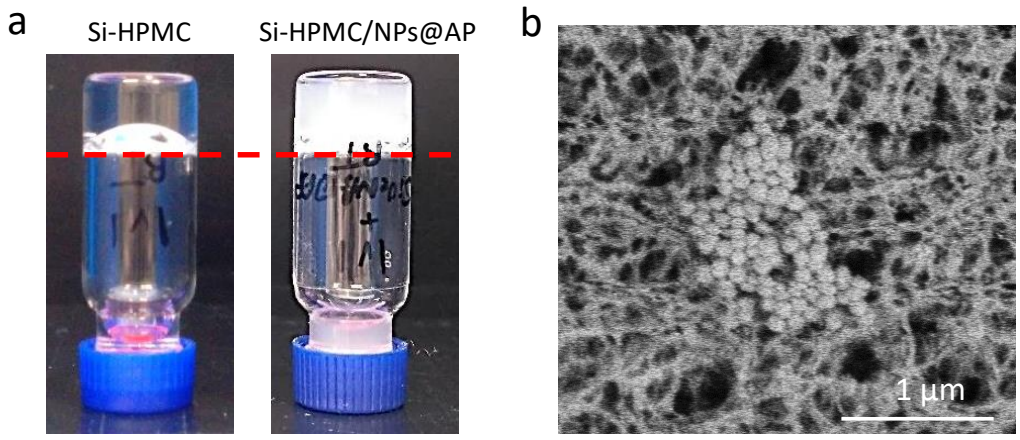

Fig. 1. (a) Inverted tube tests of Si-HPMC and Si-HPMC/NPs@AP gels after 24h. (b) Typical cryo-SEM image of Si-HPMC/NPs@AP.

The hydrogel formation was studied by oscillatory dynamic rheological measurements (Fig. S3). The elastic modulus of Si-HPMC host hydrogels (G' = 108 ± 13 Pa) is higher than the loss modulus (G'' = 8 ± 1 Pa) over all frequency range, corroborating the gel formation after 24 hours (Fig. S3a) and its mechanical stability over the time. For Si-HPMC host hydrogels with entrapped NPs@AP, even if G' (123 ± 27 Pa) is higher than G'' (10 ± 2 Pa) after 24 hours hydrogel formation (Fig. S3b), the elastic modulus increases up to G' = 185 ± 14 Pa (respect to G'' = 10 ± 1 Pa) after 48 hours to remain then stable (Fig. S3c). Therefore, the incorporation of NPs@AP enhances the mechanical properties of the host hydrogels. In both cases, the hydrogels show a linear viscoelastic regime up to 60% strain (Fig. S3d-e). We determined if AP is still active when NPs@AP are encapsulated inside the Si-HPMC hydrogel. For that purpose, the hydrogel Si-HPMC/NPs@AP was brought in contact with a solution of *para*-nitrophenyl phosphate (PNP) which is transformed in *para*-nitrophenol (λ_{max} = 405 nm) by NPs@AP embedded in the gel (Fig. S4). The catalytic activity of NPs@AP inside the Si-HPMC hydrogels is equivalent to ~0.3 µg mL^{-1} of AP

concentration free in solution. This enzyme activity is stable over 48 hours at least. Next, Si-HPMC/NPs@AP hydrogel was brought in contact with a solution of Fmoc-FF*p*Y (100 µL of 2.5 mg mL^{-1} in borax buffer 25 mM) that diffuses throughout the host hydrogel and self-assembles by enzymatic dephosphorylation caused by NPs@AP located inside the Si-HPMC hydrogel (Scheme 1b,c). The Fmoc-FF*p*Y diffusion does not produce any increase of the elastic modulus of the Si-HPMC/NPs@AP hydrogel (G' = 185 ± 19 Pa) (Fig. 2a and Fig. S5). However, it has an impact on the shear-thinning behaviour of these hydrogels, decreasing the linear viscoelastic regime region. G' remains constant and higher than G'' up to a critical deformation, γ_0 = 40 %, where G' starts to decrease until reaching the crossover point of G' and G'', moment at which takes place the change from the gel-like state to the sol-like one (Fig. 2b). Interestingly, a different rheological behavior is observed when Fmoc-FF*p*Y forms part of the hydrogel network. G" ~ 10 Pa remains constant up to 2% strain and then starts to increase reaching a maximum of 90 Pa at 30% strain followed by a decrease. This fact is indicative of a weak-strain hardening behavior related to the energy dissipation of a complex structure breakage [40].

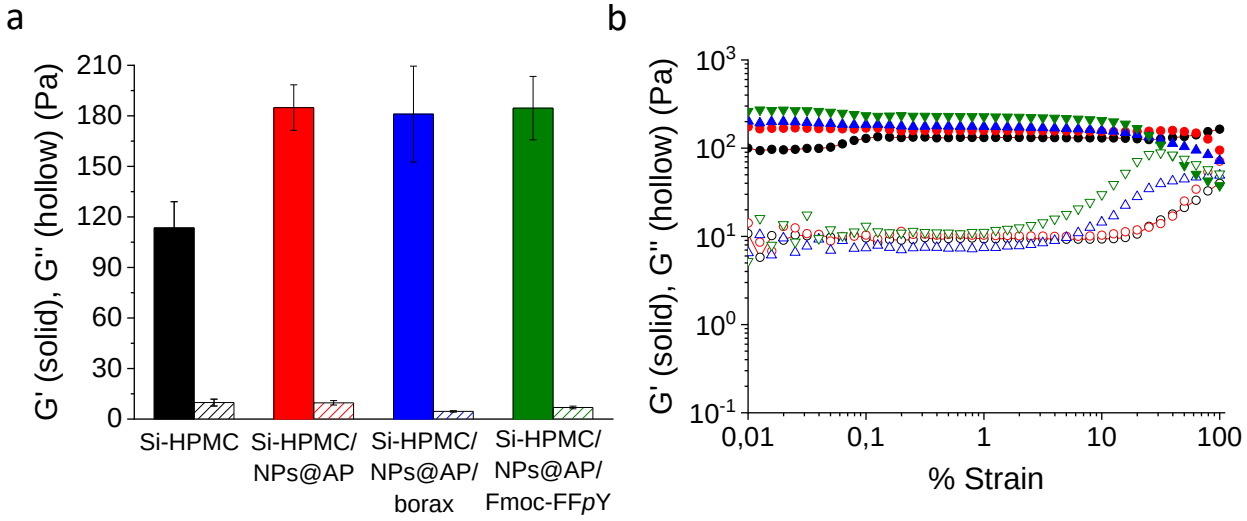

Fig. 2. Elastic modulus (G') and loss modulus (G'') of Si-HPMC (black) and Si-HPMC/NPs@AP (red) gels, and Si-HPMC/NPs@AP gels in contact with borax (blue) or Fmoc-FF*p*Y (green) (a) obtained from frequency sweeps at 1 Hz, and (b) as function of % strain.

The Fmoc-FFY self-assembly within the Si-HPMC gel was proven by attenuated total reflection Fourier transformed infrared (ATR-FTIR) spectroscopy. ATR-FTIR spectra of Si-HPMC gels containing either non-functionalized nanoparticles (NPs), named as Si-HPMC/NPs, or NPs@AP, were recorded 48h after contact with the Fmoc-FF*p*Y solution (Fig. 3a). In the case of Si-HPMC/NPs (black curve), a broad amide I band is observed in the range of 1575 – 1725 cm^{-1} that is commonly the signature of disordered amide groups (Fig. S6) [41]. For Si-HPMC/NPs@AP the appearance of a band at 1640 cm^{-1} is characteristic of aggregation via intermolecular hydrogen bonding attributed to the β-sheet structure (Fig. 3a, red line) [14, 42, 43]. The band at 1688 cm^{-1} is assigned to carbamates and consistent with a β-sheet structure and a possible anti-parallel arrangement [44]. The band centered at 1605 cm^{-1} is attributed to the deprotonated form of the terminal carboxylic acid groups [33, 45]. In addition to this, the excimer formation of Fmoc moieties from Fmoc-peptide self-assembly was monitored by fluorescence spectroscopy [26, 45]. When Si-HPMC/NPs are brought into contact with Fmoc-FF*p*Y solution, a fluorescence emission band at 317 nm due to Fmoc moieties is observed (Fig. 3b). The same emission band is observed in the case of Si-HPMC hydrogels in contact with Fmoc-FF*p*Y and without NPs embedded (Fig. S7). However, when NPs@AP are embedded inside the Si-HPMC hydrogels leading to Si-HPMC/NPs@AP, the Fmoc-FFY self-assembly takes place and a red-shift of this maximum from 317 nm towards 327 nm is observed due to Fmoc excimers formation, which is characteristic of Fmoc-FFY self-assembly [33].

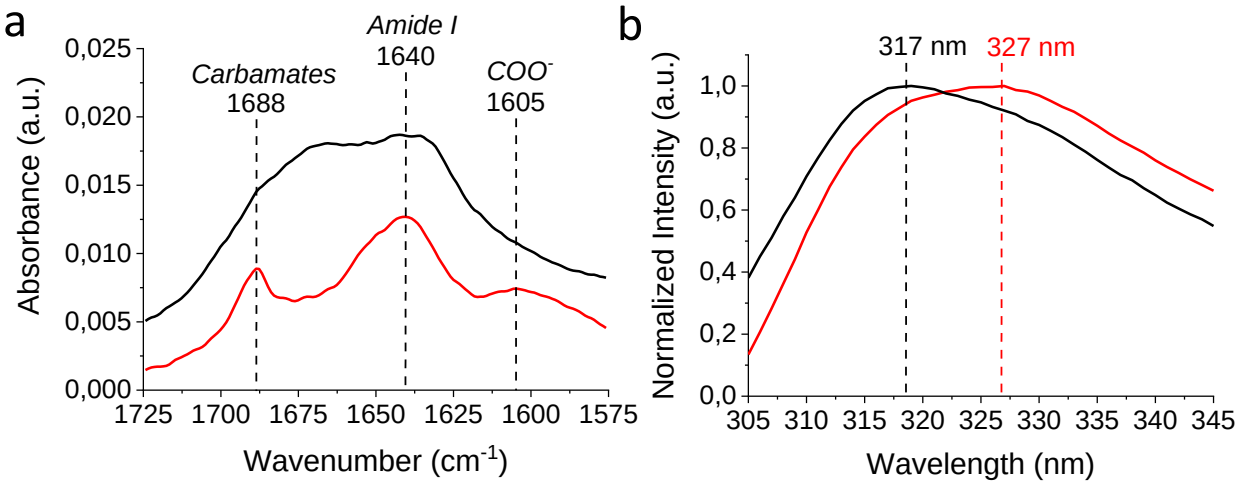

Fig. 3. (a) ATR-FTIR and (b) fluorescence emission intensity (λ_{ex}=290 nm) spectra of Si-HPMC hydrogels with naked NPs (red curve) and NPs@AP (black curve) after 48 h contact with Fmoc-FF*p*Y (2.5 mg mL^{-1}).

The supramolecular peptide self-assembly of free Fmoc-FFY within the Si-HPMC/NPs@AP host hydrogel was also visualized by confocal laser scanning microscopy (CLSM) employing Thioflavine T (ThT), a non-fluorescent probe which becomes green fluorescent when in presence of β-sheets structures [46]. NPs@AP^{RHO} incorporating 10% of rhodamine-labelled AP (AP^{RHO}, AP labelled with rhodamine B) were used to localize the AP-modified NPs, *i.e.* NPs@AP^{RHO}, in the Si-HPMC hydrogel. At the micrometer scale, the distribution of NPs@AP^{RHO} in the host material is not perfectly homogeneous (Fig. 4a) probably due to the propensity of these so-modified nanoparticles to aggregate as observed previously by cryo-SEM (Fig. 1b and S8). CLSM images show clusters (several hundred micrometre size) of NPs@AP explaining the turbidity of the resulting gel (Fig. 1b). We have first determined the mobility of the NPs@AP^{RHO} in the host gel by using fluorescence recovery after photobleaching (FRAP) measurements (Fig. S9 and Fig. S10). We found that only 11% of the particles are mobile in the gel. Because the pore size of Si-HPMC gel (~70 nm) is smaller than the NPs@AP aggregates and since all AP are covalently

bounded to the NPs, this mobility should be due to the low proportion of the smaller size NPs@AP. The diffusion of Fmoc-FF*p*Y through the Si-HPMC/NPs@AP^{RHO} hydrogel gives rise to Fmoc-FFY self-assembly revealed by the presence of ThT (Fig. 4b). The green fluorescence emission of this dye highlights the presence of Fmoc-FFY self-assembly which corresponds perfectly to the localization of NPs@AP^{RHO}. As a control experiment, Si-HPMC/ThT hydrogels without any embedded nanoparticles were brought in contact with Fmoc-FF*p*Y precursors and no fluorescence was detected (Fig. S11). It was also verified that almost no NPs@AP^{RHO} diffuse inside the Si-HPMC hydrogel when deposited on top of it (Fig. S12). The very slight diffusion of NPs@AP^{RHO} within Si-HPMC is in agreement with the 11% of mobile nanoparticles determined by FRAP measurements previously. However, the presence of clusters of NPs@AP^{RHO} before the gelation of Si-HPMC results in a gradient of NPs@AP^{RHO} distribution increasing from the bottom to the top of the host hydrogel (Fig. 4c). This is due to partial sedimentation of the NPs during the gelation. When gelation is over, the distribution of NPs@AP is fixed. Then, it is observed that when a solution of Fmoc-FF*p*Y is diffusing through this Si-HPMC/NPs@AP^{RHO}, the distribution profile of the Fmoc-FFY self-assembly (Fig. 4c) follows quite nicely the NPs@AP^{RHO} distribution. We noticed also a very slight diffusion of NPs@AP^{RHO} at the interface between Si-HPMC hydrogel and Fmoc-FF*p*Y solution, leading there to a maximum of Fmoc-FFY self-assembly. This might be due to diffusion of isolated and smaller NPs@AP^{RHO} that could constitute the 11% of diffusing NPs, as mentioned above.

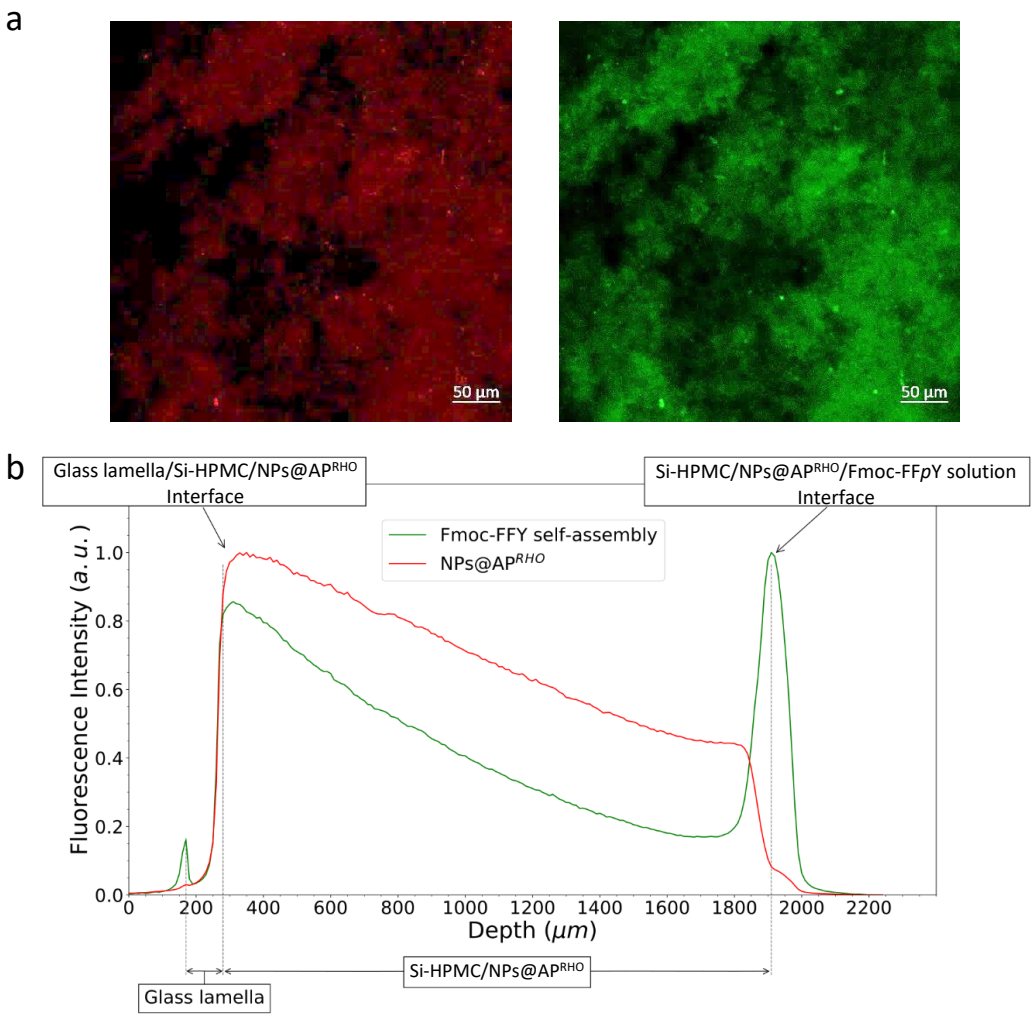

Fig. 4. (a) Confocal images, red (left) and green (right) channels of Si-HPMC hydrogels with NPs@AP embedded and distributed all around the host hydrogel. (b) Distribution profile of NPs@AP^{RHO} (red) and Fmoc-FFY self-assembly (green) observed by CLSM after the precursor peptide diffusion of Fmoc-FF*p*Y solution within a 1.6 mm thick Si-HPMC/NPs@AP^{RHO} material.

To induce the peptide self-assembly at a targeted spatial area in the host hydrogel, 1 µL of NPs@AP^{RHO} (0.6 µg mL^{-1} in borax buffer 25 mM) was injected with an adequate microsyringe through the Si-HPMC host hydrogel (Fig. 5a, 1st step) and monitored by CLSM. Subsequently, 50

µL of Fmoc-FF*p*Y (2.5 mg mL^{-1} in borax buffer 25 mM) was deposited on top of the material and let diffuse throughout the whole Si-HPMC hydrogel (Fig. 5a, 2nd step) for 24 hours: a localized green fluorescence is observed specifically in the hydrogel region in contact with the NPs@AP^{RHO} solution (Fig. 5b and S13). It thus reveals the specific spatial localization of Fmoc-FFY self-assembly due to the quasi non-diffusion of the NPs@AP^{RHO} within the Si-HPMC hydrogel. Indeed, when 1 µL of a solution of free AP^{RHO} (0.6 µg mL^{-1} in borax buffer 25 mM) was injected with a syringe in a middle point of the Si-HPMC hydrogel, a homogeneous red fluorescence observed (Fig. S14a) proves that AP^{RHO} diffuses quickly throughout the Si-HPMC hydrogel, giving rise to a homogenous green fluorescence (Fig. S14b) due to the Fmoc-FFY self-assembly.

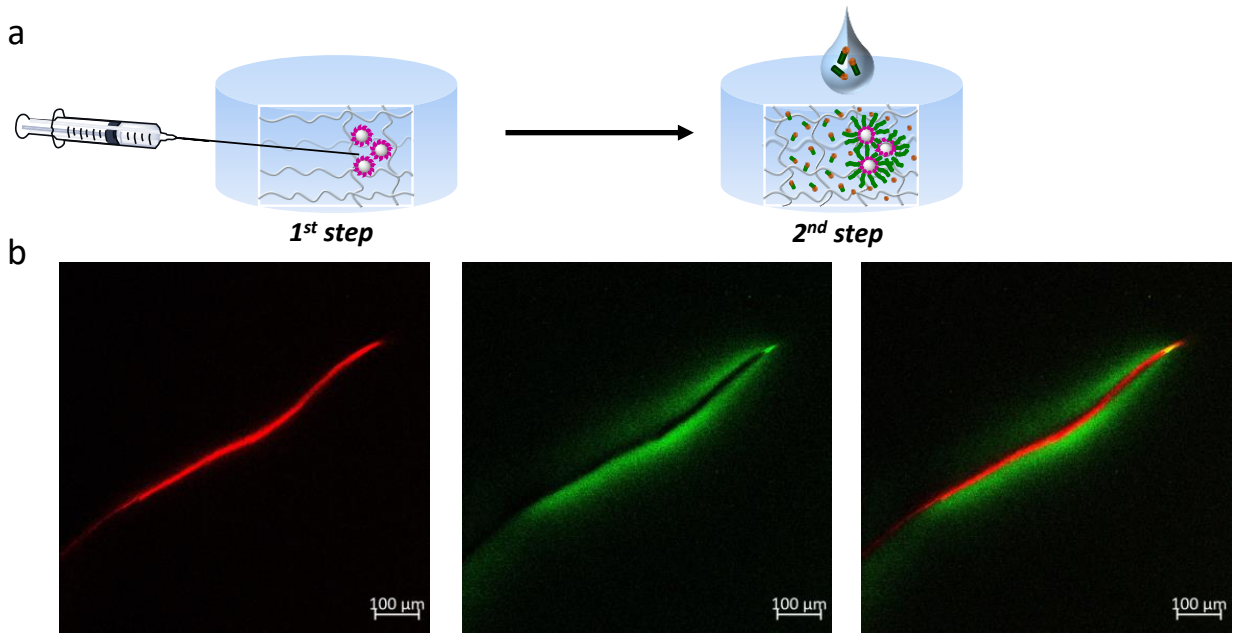

Fig. 5. (a) Scheme of the injection of NPs@AP at a targeted spatial area within the Si-HPMC host gel (1st step) and subsequent Fmoc-FF*p*Y diffusion leading to localized peptide self-assembly (2nd step). (b) Confocal images, red (left), green (center) and merged (right) channels of Si-HPMC hydrogels with NPs@AP^{RHO} localized in a specific area of the host hydrogel, after 48 h contact

with Fmoc-FF*p*Y (2.5 mg mL^{-1}) in presence of 1 mg mL^{-1} ThT. The microcrack shape in the Si-HPMC hydrogel has been created by bevelled needle.

4. Conclusions

The design of hierarchical biomaterials allows to get closer and closer to the internal structure of tissues or organs. Indeed, living matter presents non-homogeneous distributions of chemical entities and such spatial organisation is essential to ensure its function. Thus, mimicking this structuring within biocompatible polymer hydrogels is currently a hot topic. Recent work based on the concept of enzyme-assisted self-assembly has shown that the formation of self-assembling zones within chemical hydrogels can be controlled not only spatially but also temporally. The deposition of a solution of precursor peptides on the surface of the hydrogel, which contains a suitable enzyme, results in a self-assembled zone exclusively where the solution is deposited. However, this deposition also leads to diffusion of the enzyme from the host hydrogel to the precursor peptide drop, which greatly alters the width and density of the self-assembled zone within the hydrogel. To circumvent this problem, this work demonstrates that the simple use of enzymes supported by silica nanoparticles almost fully immobilises these enzymes in the gel. Furthermore, the use of a microsyringe allows the injection of very small amounts of supported enzymes into the materials, leading to spatially resolved self-assembly on the micrometre scale. We hope that these developments will be useful for the design of more complex and thus more efficient biomaterials.

ACKNOWLEDGEMENTS

Authors acknowledge the financial support received from Agence Nationale de la Recherche (EASA, ANR-18-CE06-0025-03) and from Institut Carnot MICA (DYNABIOCAT).

REFERENCES

[1] W.H. Kim, Y. Han, I.S. Lee, N.-I. Won, Y.H. Na, Development of hydrogel adhesion system for propagation of aquatic organisms, Polymer 255 (2022) 125112.
[2] M. Criado-Gonzalez, L. Corbella, B. Senger, F. Boulmedais, R. Hernández, Photoresponsive Nanometer-Scale Iron Alginate Hydrogels: A Study of Gel–Sol Transition Using a Quartz Crystal Microbalance, Langmuir 35(35) (2019) 11397-11405.
[3] Ambika, P.P. Singh, 11 - Natural polymer-based hydrogels for adsorption applications, in: S. Kalia (Ed.), Natural Polymers-Based Green Adsorbents for Water Treatment, Elsevier2021, pp. 267-306.
[4] Y. Guo, Z. Fang, G. Yu, Multifunctional hydrogels for sustainable energy and environment, Polym. Int. 70(10) (2021) 1425-1432.
[5] X. Du, J. Zhou, J. Shi, B. Xu, Supramolecular Hydrogelators and Hydrogels: From Soft Matter to Molecular Biomaterials, Chem. Rev. 115(24) (2015) 13165-13307.
[6] E. Radvar, H.S. Azevedo, Supramolecular Peptide/Polymer Hybrid Hydrogels for Biomedical Applications, Macromol. Biosci. 19(1) (2019) 1800221.
[7] Y. Tang, X. Zhang, X. Li, C. Ma, X. Chu, L. Wang, W. Xu, A review on recent advances of Protein-Polymer hydrogels, Eur. Polym. J. 162 (2022) 110881.
[8] S. Ishikawa, K. Iijima, D. Matsukuma, Y. Asawa, K. Hoshi, S. Osawa, H. Otsuka, Interpenetrating Polymer Network Hydrogels via a One-Pot and in Situ Gelation System Based on Peptide Self-Assembly and Orthogonal Cross-Linking for Tissue Regeneration, Chem. Mater. 32(6) (2020) 2353-2364.
[9] Z. Yang, H. Gu, D. Fu, P. Gao, J.K. Lam, B. Xu, Enzymatic Formation of Supramolecular Hydrogels, Adv. Mater. 16(16) (2004) 1440-1444.
[10] B. Mei, Q. Miao, A. Tang, G. Liang, Enzyme-instructed self-assembly of taxol promotes axonal branching, Nanoscale 7(38) (2015) 15605-15608.
[11] J. Gao, J. Zhan, Z. Yang, Enzyme-Instructed Self-Assembly (EISA) and Hydrogelation of Peptides, Adv. Mater. 32(3) (2020) 1805798.
[12] R.J. Williams, A.M. Smith, R. Collins, N. Hodson, A.K. Das, R.V. Ulijn, Enzyme-assisted self-assembly under thermodynamic control, Nat. Nanotechnol. 4(1) (2009) 19-24.
[13] C. Muller, A. Ontani, A. Bigo-Simon, P. Schaaf, L. Jierry, Localized Enzyme-Assisted Self-Assembly of low molecular weight hydrogelators. Mechanism, applications and perspectives, Adv. Colloid Interface Sci. 304 (2022) 102660.
[14] C. Vigier-Carrière, T. Garnier, D. Wagner, P. Lavalle, M. Rabineau, J. Hemmerlé, B. Senger, P. Schaaf, F. Boulmedais, L. Jierry, Bioactive Seed Layer for Surface-Confined Self-Assembly of Peptides, Angew. Chem. Int. Ed. 54(35) (2015) 10198-10201.
[15] J. Rodon Fores, M. Criado-Gonzalez, A. Chaumont, A. Carvalho, C. Blanck, M. Schmutz, C.A. Serra, F. Boulmedais, P. Schaaf, L. Jierry, Supported Catalytically Active Supramolecular Hydrogels for Continuous Flow Chemistry, Angew. Chem. Int. Ed. 58(52) (2019) 18817-18822.
[16] M.P. Conte, J.K. Sahoo, Y.M. Abul-Haija, K.H.A. Lau, R.V. Ulijn, Biocatalytic Self-Assembly on Magnetic Nanoparticles, ACS Appl. Mater. Interfaces 10(3) (2018) 3069-3075.

[17] R.J. Williams, T.E. Hall, V. Glattauer, J. White, P.J. Pasic, A.B. Sorensen, L. Waddington, K.M. McLean, P.D. Currie, P.G. Hartley, The in vivo performance of an enzyme-assisted self-assembled peptide/protein hydrogel, Biomaterials 32(22) (2011) 5304-5310.
[18] J. Zhou, X. Du, C. Berciu, H. He, J. Shi, D. Nicastro, B. Xu, Enzyme-Instructed Self-Assembly for Spatiotemporal Profiling of the Activities of Alkaline Phosphatases on Live Cells, Chem 1(2) (2016) 246-263.
[19] J. Rodon Fores, A. Bigo-Simon, D. Wagner, M. Payrastre, C. Damestoy, L. Blandin, F. Boulmedais, J. Kelber, M. Schmutz, M. Rabineau, M. Criado-Gonzalez, P. Schaaf, L. Jierry, Localized Enzyme-Assisted Self-Assembly in the Presence of Hyaluronic Acid for Hybrid Supramolecular Hydrogel Coating, Polymers 13(11) (2021) 1793.
[20] B. Li, M. Criado-Gonzalez, A. Adam, J. Bizeau, C. Mélart, A. Carvalho, S. Bégin, D. Bégin, L. Jierry, D. Mertz, Peptide Hydrogels Assembled from Enzyme-Adsorbed Mesoporous Silica Nanostructures for Thermoresponsive Doxorubicin Release, ACS Appl. Nano Mater. 5(1) (2022) 120-125.
[21] B. Li, A. Adam, M. Criado-Gonzalez, L. Jierry, J. Bizeau, A. Chaumont, S. Harlepp, C. Mélart, S. Begin-Colin, D. Begin, D. Mertz, Near-infrared responsive nanocomposite hydrogels made from enzyme-coated carbon nanotubes@ large pore mesoporous silica for remotely triggered drug delivery, Materialia 22 (2022) 101414.
[22] M. Lovrak, W.E.J. Hendriksen, C. Maity, S. Mytnyk, V. van Steijn, R. Eelkema, J.H. van Esch, Free-standing supramolecular hydrogel objects by reaction-diffusion, Nat. Commun. 8(1) (2017) 15317.
[23] M. Lovrak, W.E. Hendriksen, M.T. Kreutzer, V. van Steijn, R. Eelkema, J.H. van Esch, Control over the formation of supramolecular material objects using reaction–diffusion, Soft Matter 15(21) (2019) 4276-4283.
[24] L. Schlichter, C.C. Piras, D.K. Smith, Spatial and temporal diffusion-control of dynamic multi-domain self-assembled gels, Chem. Sci. 12(11) (2021) 4162-4172.
[25] H.S. Cooke, L. Schlichter, C.C. Piras, D.K. Smith, Double diffusion for the programmable spatiotemporal patterning of multi-domain supramolecular gels, Chem. Sci. 12(36) (2021) 12156-12164.
[26] M. Criado-Gonzalez, J. Rodon Fores, D. Wagner, A.P. Schröder, A. Carvalho, M. Schmutz, E. Harth, P. Schaaf, L. Jierry, F. Boulmedais, Enzyme-assisted self-assembly within a hydrogel induced by peptide diffusion, Chem. Commun. 55(8) (2019) 1156-1159.
[27] M. Criado-Gonzalez, B. Loftin, J. Rodon Fores, D. Vautier, L. Kocgozlu, L. Jierry, P. Schaaf, F. Boulmedais, E. Harth, Enzyme assisted peptide self-assemblies trigger cell adhesion in high density oxime based host gels, J. Mater. Chem. B 8(20) (2020) 4419-4427.
[28] J.-Y. Runser, M. Criado-Gonzalez, F. Fneich, M. Rabineau, B. Senger, P. Weiss, L. Jierry, P. Schaaf, Non-monotonous enzyme-assisted self-assembly profiles resulting from reaction-diffusion processes in host gels, J. Colloid Interface Sci. 620 (2022) 234-241.
[29] G. Xu, Z. Ding, Q. Lu, X. Zhang, X. Zhou, L. Xiao, G. Lu, D.L. Kaplan, Electric field-driven building blocks for introducing multiple gradients to hydrogels, Protein Cell 11(4) (2020) 267-285.
[30] X. Lyu, R. Gonzalez, A. Horton, T. Li, Immobilization of Enzymes by Polymeric Materials, Catalysts 11 (2021) 10.
[31] Q. Liu, Y. Hua, X. Kong, C. Zhang, Y. Chen, Covalent immobilization of hydroperoxide lyase on chitosan hybrid hydrogels and production of C6 aldehydes by immobilized enzyme, J. Mol. Catal. B Enzym. 95 (2013) 89-98.

[32] J. Meyer, L.-E. Meyer, S. Kara, Enzyme immobilization in hydrogels: A perfect liaison for efficient and sustainable biocatalysis, Eng. Life Sci. 22(3-4) (2022) 165-177.
[33] M. Criado-Gonzalez, J. Rodon Fores, A. Carvalho, C. Blanck, M. Schmutz, L. Kocgozlu, P. Schaaf, L. Jierry, F. Boulmedais, Phase Separation in Supramolecular Hydrogels Based on Peptide Self-Assembly from Enzyme-Coated Nanoparticles, Langmuir 35(33) (2019) 10838-10845.
[34] D. Mertz, C. Vogt, J. Hemmerlé, J. Mutterer, V. Ball, J.-C. Voegel, P. Schaaf, P. Lavalle, Mechanotransductive surfaces for reversible biocatalysis activation, Nat. Mater. 8(9) (2009) 731-735.
[35] C. Trojani, P. Weiss, J.-F. Michiels, C. Vinatier, J. Guicheux, G. Daculsi, P. Gaudray, G.F. Carle, N. Rochet, Three-dimensional culture and differentiation of human osteogenic cells in an injectable hydroxypropylmethylcellulose hydrogel, Biomaterials 26(27) (2005) 5509-5517.
[36] C. Vigier-Carrière, D. Wagner, A. Chaumont, B. Durr, P. Lupattelli, C. Lambour, M. Schmutz, J. Hemmerlé, B. Senger, P. Schaaf, F. Boulmedais, L. Jierry, Control of Surface-Localized, Enzyme-Assisted Self-Assembly of Peptides through Catalyzed Oligomerization, Langmuir 33(33) (2017) 8267-8276.
[37] J.L. Drury, D.J. Mooney, Hydrogels for tissue engineering: scaffold design variables and applications, Biomaterials 24(24) (2003) 4337-4351.
[38] W. Wang, J. Qian, A. Tang, L. An, K. Zhong, G. Liang, Using Magnetic Resonance Imaging to Study Enzymatic Hydrogelation, Anal. Chem. 86(12) (2014) 5955-5961.
[39] M. Criado-Gonzalez, M.H. Iqbal, A. Carvalho, M. Schmutz, L. Jierry, P. Schaaf, F. Boulmedais, Surface Triggered Self-Assembly of Fmoc-Tripeptide as an Antibacterial Coating, Front. Bioeng. Biotechnol. 8 (2020) 938.
[40] A. Lejardi, R. Hernández, M. Criado, J.I. Santos, A. Etxeberria, J.R. Sarasua, C. Mijangos, Novel hydrogels of chitosan and poly(vinyl alcohol)-g-glycolic acid copolymer with enhanced rheological properties, Carbohydr. Polym. 103 (2014) 267-273.
[41] X.J. Mu, K.M. Eckes, M.M. Nguyen, L.J. Suggs, P.Y. Ren, Experimental and Computational Studies Reveal an Alternative Supramolecular Structure for Fmoc-Dipeptide Self-Assembly, Biomacromolecules 13(11) (2012) 3562-3571.
[42] A.M. Smith, R.J. Williams, C. Tang, P. Coppo, R.F. Collins, M.L. Turner, A. Saiani, R.V. Ulijn, Fmoc-Diphenylalanine Self Assembles to a Hydrogel via a Novel Architecture Based on π–π Interlocked β-Sheets, Adv. Mater. 20(1) (2007) 37-41.
[43] N. Yamada, K. Ariga, M. Naito, K. Matsubara, E. Koyama, Regulation of β-Sheet Structures within Amyloid-Like β-Sheet Assemblage from Tripeptide Derivatives, J. Am. Chem. Soc. 120(47) (1998) 12192-12199.
[44] S. Fleming, P.W.J.M. Frederix, I.R. Sasselli, N.T. Hunt, R.V. Ulijn, T. Tuttle, Assessing the Utility of Infrared Spectroscopy as a Structural Diagnostic Tool for beta-Sheets in Self-Assembling Aromatic Peptide Amphiphiles, Langmuir 29(30) (2013) 9510-9515.
[45] C. Tang, R.V. Ulijn, A. Saiani, Effect of Glycine Substitution on Fmoc–Diphenylalanine Self-Assembly and Gelation Properties, Langmuir 27(23) (2011) 14438-14449.
[46] M. Biancalana, S. Koide, Molecular mechanism of Thioflavin-T binding to amyloid fibrils, Bba-Proteins Proteom 1804(7) (2010) 1405-1412.